

Tu LHR5 02

Sparse Nodes and Shallow Water - PS Imaging Challenges on the Alwyn North Field

J. Holden (CGG), D. Fritz (CGG), O. Bukola (CGG), J. McLeman (CGG), R. Refaat (CGG), C. Page* (CGG), J. Brunelliere (Total), S. Sioni (Total), A. Mitra (Total E&P UK) & X. Lu (Total E&P UK)

SUMMARY

Imaging PS-wave data acquired in the shallow water at Alwyn North with ROV-deployed ocean-bottom nodes presented particular challenges due to the sparsity of the receivers. Having ensured vector fidelity of all recorded wavefields, the processing flow made simultaneous use of the PP and PS wavefields at several junctures, including construction of the imaging velocity-depth model, requiring all wavefields to be processed in parallel and in a consistent manner. Shear-wave splitting corrections and PS demultiple were addressed to improve PS data resolution and achieve data consistency. Constructing an anisotropic velocity model based on residual move-out analysis alone was not feasible as the sparse receiver sampling resulted in poor near-offset coverage. To mitigate this full waveform inversion was used to update the P-leg velocity, and surface wave inversion for the S-leg in the crucial near-seabed interval most affected by the slowest shear velocities. Joint PP-PS non-linear tomography was used to refine this velocity model. PS-wave controlled-beam pre-stack depth migration was used extensively to assess the pre-processing as well as to validate updates to the velocity model. The resultant PS-wave data, imaged with a depth model consistent with that used for the P-wave imaging, were thus suitable for joint PP-PS elastic inversion.

Introduction

The benefits of wide-azimuth ocean-bottom seismic (OBS) for improved imaging of P-wave data – whether in shallow or deep water, with sparse or dense receiver sampling – are well documented (e.g. Arntsen and Thompson, 2003). Autonomous nodes deployed by remotely operated vehicles (ROVs) are an appropriate choice for OBS acquisition when accurate positioning of recording stations is at a premium; for example where cable-laying is hindered by infrastructure (Ronen et al., 2012). Due to operational considerations ROV-deployed surveys, such as that acquired at Alwyn North, result in sparse receiver geometries which make the estimation of near-surface properties – particularly important for accurate PS imaging – especially challenging. However, using a comprehensive workflow which combined rigorous pre-processing, an iterative use of full waveform inversion (FWI) for the P-leg velocities, surface wave inversion (SWI) for the shallow S-leg, together with a joint PP-PS non-linear tomographic inversion, an accurate velocity/anisotropic model was established which maximised the quality of the PS imaging to complement that of the PP. The resultant pre-stack depth migrated (PSDM) data were thus appropriately conditioned for joint PP-PS elastic inversion.

Data Acquisition

The data for the Alwyn North survey, located in UKCS Quadrant 3, were acquired in water depths of approximately 120 metres using over 2250 four-component ocean-bottom nodes (OBN), each containing a hydrophone sensor alongside 3 geophone sensors arranged in a Galperin configuration. These nodes were deployed in a rolling geometry that resulted in a 300 metre interval between receiver lines, and 346 metres between nodes on the same receiver line. The shot geometry initially described a shot carpet with both shotpoints and shotlines separated by 37.5 metres but operational considerations dictated an increase in the shotline interval to 50 metres mid-survey, which had to be accounted for in the data processing.

Data Processing

The objective of the data processing was not only to improve the P-wave structural imaging when compared to vintage towed streamer data over the area, but also to deliver equivalent high quality complementary PS-wave data suitable for joint PP-PS elastic inversion. This objective would be achieved partly through construction of an anisotropic velocity-depth model for both P-wave and S-wave velocities with a common anisotropic description, and in part through high-end signal processing of the P-wave data and the PS-wave data. Particular challenges for the converted-wave processing included solving for the effects of near-seafloor velocity anomalies, exacerbated by the lower velocities experienced by the upgoing S-leg of the converted wavefield, and poor data coverage resulting from the sparse receiver deployment. The lack of coverage apparent for the P-wave case was exaggerated for the PS case due to the conversion point occurring towards the node location and away from the geometrical midpoint. Other PS issues to be addressed included correcting for shear-wave splitting, and removing the effects of multiples beneath the Base Cretaceous Unconformity (BCU).

Vector Fidelity

A critical step in OBN processing is to ensure vector fidelity for both the PP as well as the PS data. In the case of the data recorded at Alwyn North the 3 geophone components were rotated from their initial Galperin configuration to a north/east/down system, and corrected for tilt and heading taken from in situ measurements before a data-driven correction for residual rotation. The direct arrivals were also used to derive a global correction for systematic ‘source drag-back’, accounting for the difference between the reported GPS source position and the centre of the source energy, and to reposition all receiver components. The receiver repositioning analysis, which used an algorithm insensitive to clock-drift, indicated that 99% of all nodes were within 5 metres of the locations reported by the acquisition contractor. After application of positioning corrections the data were assessed for clock-drift, and corrected where necessary. The horizontal components were then rotated to the radial-transverse coordinate system for further processing.

PS-Wave Pre-processing

A fundamental step for PS-wave processing is the correction of any shear-wave splitting that may be observed in the data due to the presence of azimuthal anisotropy (Granger et al., 2001). The data from Alwyn North were analysed for such birefringence corrections at the Top Skade horizon (Figure 1), which was the shallowest horizon that demonstrated the typical PS response to horizontally transverse isotropic media. Short-offsets were selected from both radial and transverse receiver gathers, azimuthally sectorised (24 sectors of 15 degrees), and stacked after application of normal moveout (NMO). The resulting gathers exhibited the characteristic periodic arrival times of the event on the radial component, and the polarity reversals separated by quiescent sectors on the transverse component (Figure 1a to 1d). After appropriate editing of the derived anisotropy attributes the data were rotated into the two principal axes describing the ‘fast’ direction (the isotropy plane) and the ‘slow’ direction (the symmetry-axis plane) prior to compensating the ‘slow’ data to account for the later arrival times. The fast and time-aligned slow components, now corrected for overburden anisotropy, were then rotated back to the radial and transverse system. The corrected data showed little evidence of a change in the anisotropic regime for the deeper data (Figure 1e to 1f), and from this point the transverse data were discarded.

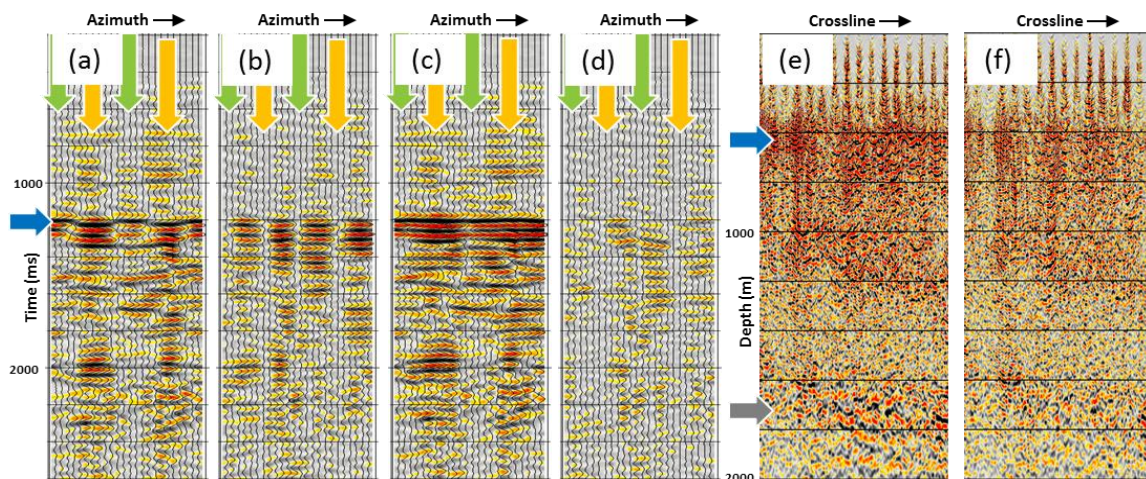


Figure 1 Common-receiver gather split into NMO-stacked azimuth sectors; (a) radial, (b) transverse, (c) radial after overburden correction, (d) transverse after overburden correction. The blue arrow indicates the analysed horizon (Top Skade). Green arrows indicate the fast anisotropic axis, and orange arrows indicate the slow axis. Note the removal of energy from the transverse component and the resultant improved coherency, energy and flatness on the corrected radial gather. The PSDM of the transverse component for an inline (e) before shear-wave splitting correction, and (f) after correction, show a reduction of energy at the analysis horizon (blue arrow) as well as in the deeper section (grey arrow).

Other key processes included denoising the data in a manner consistent with the P-wave data, and a cascaded approach to removing multiples. The demultiple flow included removal of source-side water-layer related multiples, as well as longer period free-surface multiples on the downgoing P-leg, which were modelled and adaptively subtracted from the PS data. Whilst the multiple contamination on the PS data is less severe than for the P-wave data, the demultiple process nonetheless gave a significant improvement to the interpretability of the migrated events below the BCU (Figure 2). Further notable processing steps included the simultaneous analysis of P-wave and PS-wave data for surface-consistent properties, including joint solutions for surface-consistent amplitudes (Henin et al., 2014), as well as surface-consistent residual statics using a non-linear scheme based on a Monte-Carlo method coupled with simulated annealing (Le Meur and Poulain, 2012). Source-side deghosting of the PS wavefield was also applied, to be coherent with the P-wave processing.

Test lines were routinely migrated in common-receiver gathers with a PS-wave controlled-beam migration (CBM) algorithm which enabled results to be assessed in the depth image domain. This also allowed direct structural comparisons to be made with equivalent depth-migrated PP data (Figure 3).

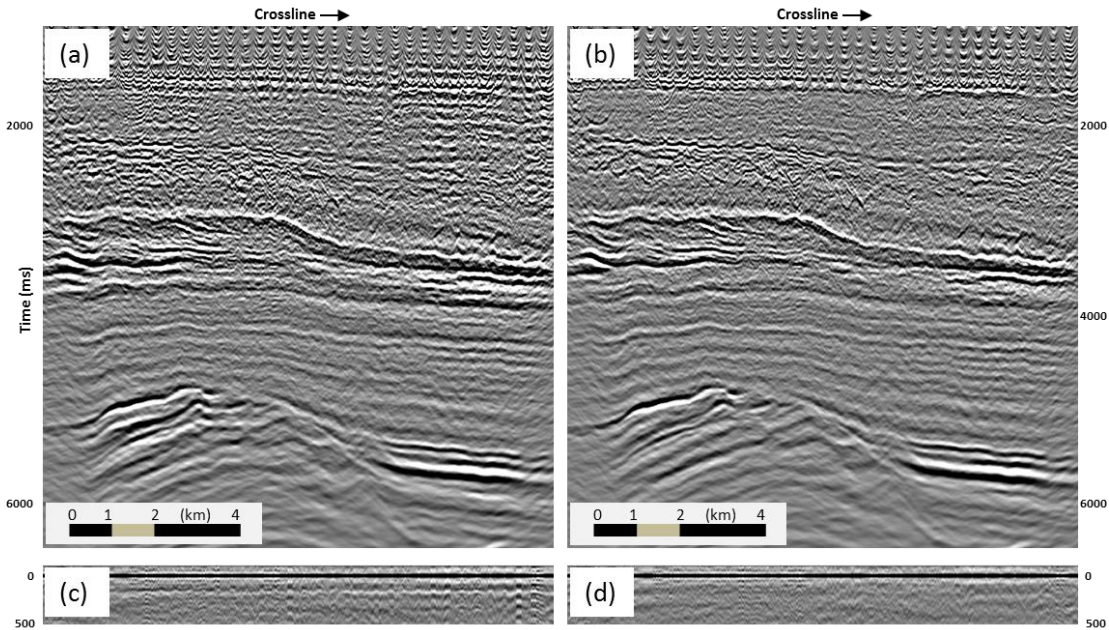


Figure 2 PS-wave PSDM converted to PS time; inline (a) before demultiple, (b) after demultiple processing, (c) autocorrelation before demultiple, (d) autocorrelation after demultiple. Note the improved resolution of the tilted fault blocks below the BCU, at approximately 5000 ms, and the suppression of the periodicity on the autocorrelation after demultiple.

PP-PS Depth Model Building and Imaging

One of the principal objectives of the project was to construct a depth velocity model to satisfy the imaging requirements of both PP and PS wavefields. A priori information was available for the P-leg from legacy towed-streamer processing conducted in 2010. This initial P-velocity (V_p) model was then updated through 4 passes of FWI, using progressively longer offsets and higher frequencies (up to 12 Hz) to model the shallow P-leg velocities with increasing resolution. In the absence of adequate shear sonic logs within the OBN survey area, the initial S-velocity (V_s) model was constructed from more complete well information that was 13 km distant. Horizon markers and event interpretations were used to extrapolate from these wells within a stratigraphic framework, and the result assessed using the available logs from within the OBN area. PP-PS event registration was then used to update V_s , and a scan of epsilon in the shallow section used to improve PS resolution whilst retaining registration with the equivalent P-wave events. V_p was further updated with a non-linear joint tomography using demigrated kinematic invariants (Guillaume et al., 2013) from both upgoing and downgoing PP wavefields, before V_s and epsilon were jointly updated with additional invariants derived from the PS-wave data. PS-wave CBM was used consistently throughout the model-building process to validate results, benefiting from the improvement in signal to noise ratio inherent to this algorithm (Casasanta and Gray, 2013).

The results of a surface (Scholte) wave inversion, which added detail to the very near-surface shear velocity estimate, were introduced at a relatively late stage in the model-building process. This necessitated a revision to the surface-consistent residual statics, after replacing the initial primary shear receiver statics with a model derived from the accumulated vertical traveltimes through the SWI model. A further scan was performed to update epsilon and improve focusing, whilst retaining delta to maintain the well calibration, and hence the gross PP-PS event registration. Finally, V_s was updated with non-linear tomography using all the available attributes derived from the PS wavefield, downgoing ('mirrored') PP, and conventional upgoing PP wavefields.

The resultant depth-imaged PS data were thus appropriately conditioned for joint analysis with the PP data, such as a joint PP-PS elastic inversion scheme which can estimate rock properties with more accuracy than a PP-only approach (Barnola and Ibram, 2012).

Conclusion

A comprehensive workflow was used to overcome the challenges imposed on imaging PS-wave data recorded with a sparse node geometry in shallow water. Careful pre-processing of all recorded data was essential both for the model building and final imaging. Whilst FWI aided the estimation of the P-wave velocities, SWI added detail to the shallowest shear velocities which would be difficult to recover from tomographic analysis alone. Joint PP-PS non-linear tomography utilised information from all the recorded wavefields to update the final model. The resulting PS-imaged data were appropriately conditioned for a joint PP-PS elastic inversion to derive more accurate estimates of rock properties than may be obtained from PP data alone.

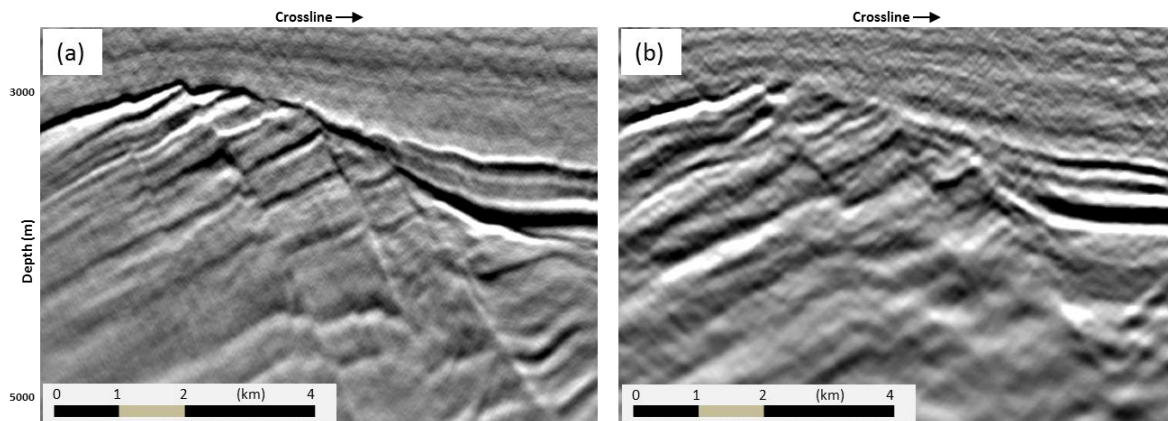


Figure 3 Comparison of imaged wavefields: (a) P-wave Kirchhoff PSDM; (b) PS-wave CBM PSDM with post-migration Q_{ps} amplitude compensation ($Q_{ps}=115$). An intermediate velocity model is used.

Acknowledgement

The authors wish to thank CGG and Total Exploration & Production UK for permission to publish, and acknowledge the dedication of the CGG and Total staff who were involved in the processing.

References

- Arntsen, B. and Thompson, M. [2003] The importance of wide azimuth in imaging. *65th EAGE Conference & Exhibition*, Extended Abstracts.
- Barnola, A.-S. and Ibram, M. [2012] 3D Simultaneous Joint PP-PS AVO Seismic Inversion in Schiehallion Field, UKCS. *74th EAGE Conference & Exhibition*, Extended Abstracts.
- Casasanta, L. and Gray, S. [2013] Converted-wave Controlled Beam Migration with Sparse Sources or Receivers. *75th EAGE Conference & Exhibition*, Extended Abstracts.
- Granger, P.-Y., Bonnot, J.-M., Gresillaud, and A., Rollet, A. [2001] C-wave resolution enhancement through birefringence compensation at the Valhall Field. *71st Annual International Meeting, SEG*, Expanded Abstracts, 772-775.
- Guillaume, P., Zhang, X., Prescott, A., Lambare, G., Reiner, M., Montel, J.P., and Cavalie, A. [2013] Multi-layer non-linear slope tomography. *75th EAGE Conference & Exhibition*, Extended Abstracts.
- Henin, G., Garceran, K., Le Meur, D., Bertin, F., and Rollet, A. [2014] Surface-Consistent Amplitude Simultaneous Inversion for PP and PS Data. *76th EAGE Conference & Exhibition*, Extended Abstracts.
- Le Meur, D., and Poulain, G. [2012] Joint estimation for P-P and P-S Residual Statics. *74th EAGE Conference & Exhibition*, Extended Abstracts.
- Ronen, S., Rokkan, A., Bouraly, R., Valsvik, G., Larson, L., Ostenvig, E., Paillet, J., Dynia, A., Matlosz, A., Brown, S., Drummie, S., Holden, J., Koster, K., Monk, D. and Swanton, M. [2012] Imaging shallow gas drilling hazards under three Forties oil field platforms using ocean-bottom nodes. *The Leading Edge*, 31(4), 465-469.